Physics Procedia

Volume 75, 2015, Pages 1011–1021

20th International Conference on Magnetism

Thickness dependent properties of Sr_2FeMoO_6 thin films grown on $SrTiO_3$ and $(LaAlO_3)_{0.3}(Sr_2AlTaO_6)_{0.7}$ substrates

I. Angervo[1], M. Saloaro[1]*, H. Palonen[1], S. Majumdar[1,2], H. Huhtinen[1], and P. Paturi[1]

[1] Wihuri Physical Laboratory, Department of Physics and Astronomy, University of Turku, FI-20014 Turku, Finland

[2] NanoSpin, Department of Applied Physics, Aalto University School of Science, P.O. Box 15100, FI-00076 Aalto, Finland

Abstract

Pure, fully textured and *c*-axis oriented Sr_2FeMoO_6 films were deposited on $SrTiO_3$ and $(LaAlO_3)_{0.3}(Sr_2AlTaO_6)_{0.7}$ substrates with different thicknesses. A decrease in substrate induced strain was observed in films on $SrTiO_3$ with increasing thickness, but the strain in the films on $(LaAlO_3)_{0.3}(Sr_2AlTaO_6)_{0.7}$ was nearly constant within the whole film thickness range. Despite the differences in the strain, the magnetic properties of the films showed similar thickness dependence on both substrates. The saturation magnetization and Curie temperature increased until around 150 nm thickness was reached. Semiconducting low temperature upturn in resistivity was observed in all the films and it was enhanced in the thinnest films. Thus, the band gap energy increases with increasing film thickness. According to these results, at least 150 nm thickness is required for high quality Sr_2FeMoO_6 films.

Keywords: SFMO, Thin films, Strain, Saturation magnetization, Curie temperature, Spin channel system, Energy gap

1 Introduction

Since Kobayashi *et al.* discovered the magnetoresistive behaviour in polycrystalline Sr_2FeMoO_6 (SFMO) samples [1], intensive research has taken place to understand the mechanisms behind the magnetic and resistive phenomena. Magnetoresistive behaviour, high Curie temperature, T_C, around 410–450 K [1], and high spin polarization make double perovskite SFMO an extremely valuable candidate for future spintronic and magnetoresistive applications. Fabrication of SFMO thin films is a delicate process and formation of parasitic impurity phases can diminish the properties of the SFMO films. Common impurities found in SFMO are Fe and $SrMoO_4$

*Corresponding author, email: minnamari.saloaro@utu.fi

Selection and peer-review under responsibility of the Scientific Programme Committee of ICM 2015

doi:10.1016/j.phpro.2015.12.170

[2, 3]. Also antisite disorder (ASD) and oxygen vacancies are strong factors affecting the magnetic properties. ASD refers to disorientation in SFMO lattice structure where Fe has changed positions with Mo.

Pulsed laser deposition (PLD) has proven to be an excellent method for SFMO thin film fabrication. One of the obvious attributes for thin films is the choice of substrate material and film thickness. Previous publications show substantial effect of substrate induced lattice mismatch and film thickness on structural, magnetic and resistive properties of SFMO films [4, 5, 6, 7, 8, 10, 11]. Strain in thin films usually becomes relaxed towards the bulk lattice parameter values with the increase of film thickness [5, 4, 11]. This is why strain is usually more significant in thinner films. Structural relaxation can also happen through dislocations. On MgO substrate with strong tensile strain, Boucher and Jalili *et al.* reported nearly a constant value a and/or c lattice parameter through the whole thickness range [5, 7]. The constant c might be due to the reorganization of SFMO film on MgO substrate where the relaxation might occur through other defects, not only by the relaxation of strain with increasing film thickness [5, 7].

Some of the used substrates with different lattice mismatches have been MgO, $SrTiO_3$, $Sr_{0.5}Ba_{0.5}TiO_6$, $LaAlO_3$ and $NdGaO_3$ [6, 8, 10] and it has been reported that thicker films and/or smaller lattice mismatch between substrate and film result in higher magnetization values [6, 8]. Magnetization can be reduced due to ASD and oxygen vacancies [12, 13]. Also parasitic impurity phases can affect the magnetization [11, 14]. In our previous paper [11], we have observed a possible increase of impurity phase with increasing film thickness. This was argued to be a possible explanation for decrease in T_C.

An upturn at low temperatures in resistivity temperature measurements indicates semiconducting behaviour and this has been observed in various earlier reports [10, 11, 15, 16]. Semiconducting behaviour is reported to be stronger in films with larger lattice mismatch and smaller film thickness [10, 11]. Semiconducting behaviour appears to be linked to the changes in SFMO band structure and it has been reported that strain may affect the band structure [4, 17]. Changes in the band structure induced by strain could be a direct consequence of shorter Fe-Mo-Fe bonds [4]. The band structure is also affected by imperfections like ASD and oxygen vacancies. It has been shown that ASD and oxygen vacancies can reduce the band gap and halfmetallicity can be lost in SFMO [18, 19].

Despite the valuable research, there is still much to do in order to fully understand the phenomena observed in SFMO thin films. The effect of substrate and/or film thickness on structural and magnetic properties of SFMO films have been reported [4, 5, 7, 8, 10, 11]. The amount of research that systematically studies the effect of film thickness is rather limited and further investigation is needed. In this paper, we have investigated the effects of substrate induced strain, and its relaxation with film thickness, on structural, magnetic and resistive properties of SFMO thin films.

2 Experimental details

SFMO target for pulsed laser deposition (PLD) was made from nanograined powder, which was prepared by sol-gel method, and the details have been reported elsewhere [3, 20]. Two sets of SFMO thin films with different thicknesses were deposited with PLD on two different single crystal substrate materials, $SrTiO_3$ (STO) (001) and $(LaAlO_3)_{0.3}(Sr_2AlTaO_6)_{0.7}$ (LSAT) (001) in Ar-atmosphere in 9 Pa pressure. Temperature of the substrate during the deposition was 1050 °C. Thickness of the films was controlled by the number of pulses and the thicknesses were calibrated by using cross-sectional high-resolution transmission electron microscopy (HRTEM)

imaging (JEOL JEM-4010 at a accelerating voltage of 400 kV) [21]. The average thickness of the SFMO films with 2000 pulses on STO substrate was measured as 160 nm and on LSAT as 140 nm. Therefore by assuming a linear growth within this thickness range, an average deposition rates of SFMO were estimated as 0.8 Å/pulse on STO and 0.7 Å/pulse on LSAT, respectively. For the used pulse numbers of 500, 1000, 1500, 2000, 5000 and 10000, the thicknesses are 40, 80, 120, 160, 400 and 800 nm for films on STO, and 35, 70, 105, 140, 350 and 700 nm for films on LSAT. For the error analysis, the error for 160 nm thick SFMO film thickness was estimated to be approximately ±10 nm. Equal relative difference was assumed in all our films.

The structural characterization was done with X-ray diffraction using Philips X'Pert Pro MPD diffractometer with Schulz goniometer. $\theta - 2\theta$-scans were made between 20° and 114° to check possible impurity phases and to obtain the c-lattice parameters. Peak (336) was measured separately with detailed $\theta - 2\theta$ scan to determine the a-lattice parameter. The strain is obtained from lattice parameters. Texture analysis was conducted by measuring the SFMO (204) peak with $\phi - \psi$-scans. Substrate peaks were used as an internal standard.

The magnetic properties were investigated using MPMS XL SQUID magnetometer by Quantum Design. The field-cooled (FC) and zero-field-cooled (ZFC) magnetizations were measured in 100 mT field as a function of temperature between 10 K and 400 K. FC magnetization results were used to determine the T_C specified as a minimum of the derivative of the FC curve. Magnetization irreversibility M_{irr} was calculated as a difference between FC and ZFC curves defined as $M_{irr} = M_{FC}(10K) - M_{ZFC}(10K)$. Hysteresis loops were measured between ± 500 mT at 10 K, 100 K, 300 K and 400 K. The saturation magnetization was evaluated from the hystersis loop measured at 10 K. Coercivity, determined as an average of the absolute values, was obtained by observing the external field for zero magnetization in 10 K hysteresis loop. Resistive properties of SFMO films were measured by Quantum Design Physical Property Measurement System (PPMS). Resistivity in different magnetic fields of 0 T, 50 mT, 100 mT, 500 mT, 1 T and 5 T was recorded as a function of temperature from 10 K to 350 K.

3 Results and discussion

3.1 Structural analysis

The $\theta - 2\theta$ scans and pole figures are presented in Fig. 1. $\theta - 2\theta$ results are shown for the thickest and the thinnest films on both STO and LSAT and for 160 nm thick film on STO and 140 nm thick film on LSAT. Pole figures of the texture analysis are shown for 160 nm thick SFMO film on STO and 140 nm thick film on LSAT. In $\theta - 2\theta$ scans, $(00l)$ peaks are observed for both SFMO and substrates, but no peaks of any typical impurities are observed. However, XRD measurements are not able to show possible impurity phases below 1% of the total volume. The small peaks seen around 44° and 52° arise from the sample holder. Because of the crystal structure and high texture of SFMO films, only (132) and (204) peaks are visible in pole figures. Besides the change in the intensities due to the different thicknesses, there are no distinguishable differences between the films. According to XRD measurements, films are phase pure, fully texturized and c-axis oriented.

To estimate the strain in our films, we determined the lattice parameters of SFMO thin films. An asymmetric Gaussian function was fitted to peaks to obtain the peak positions used in the determination of lattice parameters. The c-parameter was determined with the Nelson-Riley method using SFMO (002), (004) and (008) peaks in $\theta - 2\theta$-scan [22]. The a-parameter was determined using (336) peak position with Bragg law. The relative difference in the lattice cell volume, $\Delta V(\%) = (a^2 c - V_{ref})/V_{ref}$, was calculated from lattice parameters. As a reference

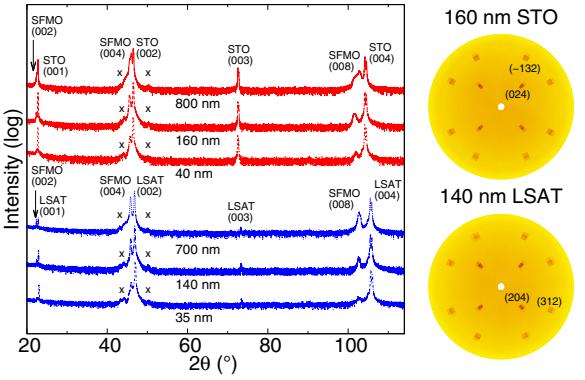

Figure 1: The room temperature XRD $\theta - 2\theta$ diffractograms of selected film thicknesses with identified SFMO $(00l)$ peaks on both STO and LSAT substrates. The pole figures of the texture scans are given with relative intensities measured at $2\theta = 57.106°$ for (204) and (132) peaks of SFMO films with thicknesses of 160 nm for STO and 140 nm for LSAT, respectively. Peaks marked with "x" arise from the sample holder.

for V_{ref}, we used the lattice cell volume of the polycrystalline bulk sample lattice parameters, $a_{\mathrm{bulk}} = 5.575$ Å and $c_{\mathrm{bulk}} = 7.893$ Å, reported by Nakamura *et al.* [23]. The results for the a- and c-parameters and ΔV are shown with error bars as a function of film thickness in Fig. 2(a). The errors for lattice parameters are obtained as standard deviation from the assymetric Gaussian function fit. The lattice parameter a for the films on STO decreases when the film thickness increases up to 120 nm. Once the thickness is approximately 120 nm, the a-parameter slightly increases. The c-parameter has an opposite dependence with the film thickness when compared to a-parameter in films on STO. The a- and c-parameters for films on LSAT have a constant value, 5.60 Å and 7.89 Å, within the error limits through the whole thickness range. As shown in Fig. 2(a) for both substrates, the film thickness has similar effect on the relative volume difference as previously observed for a-parameter. The absolute values for lattice parameters are close to previously published values [4, 5, 7, 8, 11]. We have previously observed an increase in a and decrease in c lattice parameter when SFMO film thickness increases on STO [11]. The results here on STO do not fully follow similar tendency and especially the thinnest films seem to deviate from the earlier results.

The results from the strain calculations are presented in Fig. 2(b) with error bars. Strain was determined using both a- and c-parameters according to the formula $\varepsilon_{\mathrm{a}} = (a_{\mathrm{film}} - a_{\mathrm{bulk}})/a_{\mathrm{bulk}}$. Obviously, the results indicate the same dependence between strain and film thickness which was observed between lattice parameter and film thickness for SFMO thin films on both substrates. Films deposited on STO show negative compressive in-plane strain as expected due to negative lattice mismatch. The films on LSAT show close to zero ε_{c} and small positive ε_{a}. Due to the negative lattice mismatch, around -1.88 %, between the LSAT substrate and SFMO, one would expect negative ε_{a}. Similar results for SFMO films deposited on MgO has been reported and it was suggested that this can be explained through reorganization of SFMO films near the interface [5, 7]. Based on the constant in-plane strain, SFMO lattice parameters on STO show possible relaxation in films with thickness above 160 nm. However, all the films on LSAT seem to be fully relaxed. Previously SFMO films on STO have been reported being fully relaxed in

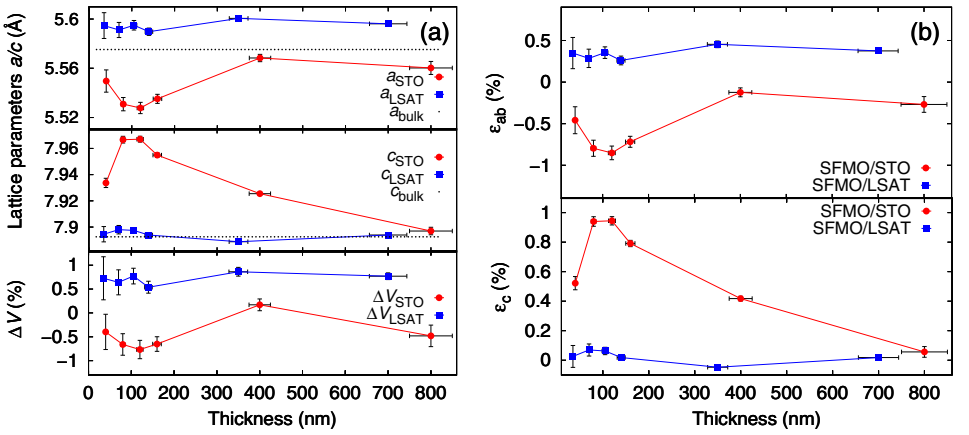

Figure 2: The film thickness dependence of the room temperature lattice parameters a/b and c, and the unit cell volulme difference as compared to the bulk value of 245.32 Å^3 [23] (a), as well as the substrate induced strain in a and c directions (b) calculated from the XRD 2θ data for SFMO films on STO and LSAT substrates. X- and y-error bars are included for lattice parameters, relative volume change, strain and thickness.

films with 80 nm thickness [4]. On the other hand, Boucher *et al.* have reported no relaxation in SFMO films with thickness higher than 100 nm [5].

3.2 Magnetic properties

Fig. 3 presents an example of the hysteresis loop between ±210 mT and temperature dependence of ZFC/FC magnetization obtained from SFMO film with 160 nm thickness deposited on STO substrate. The inset in Fig. 3(b) shows the first order derivative of the FC curve, which is used to determine T_C. The saturation magnetization, M_s, and the coercivity, B_c, obtained from hysteresis loops at 10 K for different films are presented in Fig. 4(a) with error bars as a function of film thickness. The error bars for M_s are obtained by estimating the error in thin film volume. For B_c, the error bars are obtained from SQUID resolution. Until film thickness reaches approximately the value of 100 nm on both STO and LSAT, M_s increases with film thickness. Above this thickness, the saturation magnetization can be considered constant within the error limits being around 2.3 μ_B/f.u. in films on both substrates. Since ASD has been observed to have significant effect on M_s and oxygen vacancies may also decrease M_s [12, 13], we could assume higher amount of these defects in thinner films. Similar tendency can be observed in coercivity field. The B_c values decrease with increasing film thickness and after thickness of ∼150 nm they reach a constant value. However, the B_c of SFMO films on LSAT decreases slightly even after film thickness has reached over 150 nm value. This could be related to grain boundaries and dislocations that may arise from lattice mismatch, being most likely linked to our coercivity results since structural defects cause magnetic domain pinning [24]. SFMO films on LSAT show higher B_c values compared to films on STO. This is expected due to dislocations and structural defects caused by the larger lattice mismatch.

The Curie temperatures determined from the FC curves are presented as a function of film thickness in Fig. 4(b) with error bars. The error bars are obtained by evaluating the

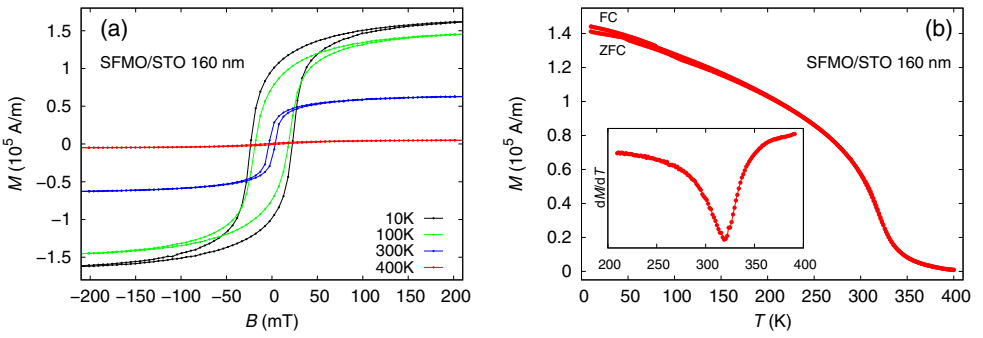

Figure 3: (a) Hysteresis loops measured at different temperatures and (b) temperature dependence of ZFC/FC magnetization of 160 nm thick SFMO film deposited on STO. Inset in (b) shows the first order derivative of FC curve, which is used to determine T_C.

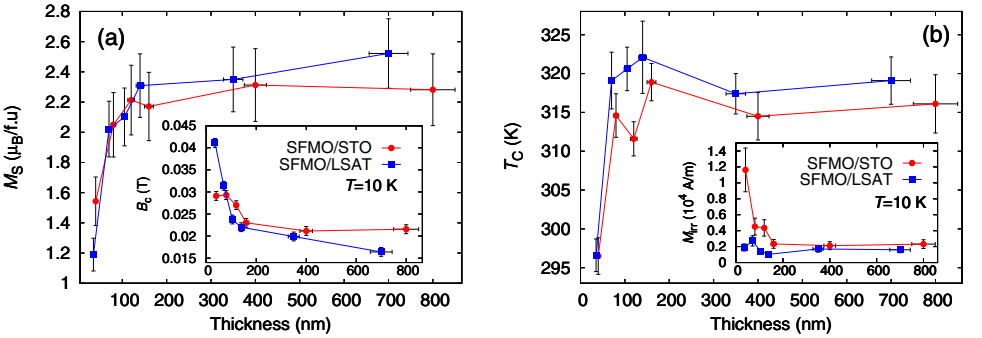

Figure 4: (a) Thickness dependence of the saturation magnetization M_s defined in the field of 400 mT (main panel) and the coercivity field B_c (inset) determined from the hysteresis loops at 10 K. X- and y-error bars are included for M_s, B_c and thickness. (b) The Curie temperature T_C and the magnetic irreversibility (inset) defined as $M_{irr} = M_{FC}(10K) - M_{ZFC}(10K)$ as a function of film thickness with error bars.

temperature range of derivative values around the minimum of the first order derivative of FC curve. First T_C increases rapidly from the thinnest film to approximately 80 nm thick film on STO and 70 nm thick film on LSAT and the increasing tendency continues until the approximate 160 nm thickness on STO and 140 nm thickness on LSAT is reached. Results also show that there is a shallow downturn in T_C in films on both substrates with the two thickest films. However, considering the error limits, significant change in T_C on both substrates is only observed between the thinnest film and the others. We have observed a similar downturn tendency between film thickness and T_C in our previous paper [11]. It was concluded that decrease in T_C might be due to a possible impurity phase that is formed in thick films, but no indication of such impurity phases was observed here. From our SFMO films, the highest T_C value is approximately 319 K on STO and 322 K on LSAT. The T_C values are similar to the results reported earlier [10, 14, 25]. However, the method of how T_C is determined varies in literature which makes comparison of values difficult.

Since FC and ZFC curves deviate from each other at low temperatures, we present the results for M_{irr} in the inset of Fig. 4(b) with error bars. The error bars are obtained by estimating the error in thin film volume. Once film thickness increases, M_{irr} decreases in films on STO, having a constant value above 150 nm thickness. SFMO films on LSAT show similar tendency in M_{irr} with smaller deviation. Deviation of FC and ZFC magnetization at low temperatures is linked to the magnetic domain structure and domain pinning [26]. For SFMO films in general, this suggests existence of impurities or dislocations especially for the thinnest films. Because our XRD results show that our films are impurity free, the dislocations are more likely to explain the magnetic results [9].

Strain and sample inhomogeneties are linked to lattice mismatch which has been shown to be strongly related to ASD [8]. Since the results for the films on STO show correlation between strain and magnetic results, we conclude that the higher strain in the thinnest films disturbs the magnetic ordering possibly by changing Fe-Mo-Fe bond angles and through ASD and oxygen vacancies, thus decreasing T_{C} and M_{s}. Sample inhomogeneties and dislocations induced by the strain can also explain our B_{c} and M_{irr} results in thin films through domain pinning. However, the correlation between the structural analysis and the magnetic measurements is not clear, especially in the thinnest films, where more mechanisms, such as low-angle grain boundaries, explain our results. The small positive strain in SFMO films on LSAT substrates implies that some kind of reorganization or over-relaxation due to the higher compressive lattice mismatch occurs at the interface. Therefore, the results for the films on LSAT can be understood through reorganization of the film at the interface [5, 7]. Reorganization happens near the interface region where dislocations relax the strain between the substrate and the film. In the interface region, film grows with high amount of defects. After reorganization, SFMO film grows with only a few defects, dislocations, ASD and oxygen vacancies. Therefore, the effect of reorganization on magnetic properties comes less apparent in thicker films and results in similar tendency as observed in films on STO.

3.3 Temperature dependence of resistivity

Insets in Fig. 5(a) and (b) show the change of the resistivity of 40 nm thick SFMO film on STO and 35 nm thick film on LSAT as a function of temperature measured in 0.05 T, 1 T and 5 T external magnetic fields. Since the temperature dependencies in different fields differ little, we have shown the change of the resistivity as a function of temperature in 1 T for the films with different thicknesses on STO (a) and on LSAT (b) in the main panel of Fig. 5. The change of the resistivity $\Delta\rho$ was calculated according to the formula $\Delta\rho = (\rho_{\mathrm{T}} - \rho_{\mathrm{min}})$, where ρ_{T} is the resistivity at temperature T and ρ_{min} is the resistivity minimum within the measured temperature range. Results show a clear low temperature upturn in resistivity with 40 nm film on STO and 35 nm film on LSAT when the temperature is decreased below 100 K indicating semiconducting behaviour. Altough the upturn is much larger in the thinnest films, it is still observerd in all the films. From the resistivity temperature dependence in 0 T, we determined the temperature $T_{\rho\mathrm{min}}$ defined here as a temperature of minimum resistivity. Results for $T_{\rho\mathrm{min}}$ with error bars are shown in Fig. 6(b). The error bars for $T_{\rho\mathrm{min}}$ are based on the temperature resolution in PPMS. $T_{\rho\mathrm{min}}$ is higher in thinner films and decreases with increasing film thickness. $T_{\rho\mathrm{min}}$ has a constant value in films with thickness above approximately 100 nm on both STO and LSAT.

In previous paper we have used a semiempirical model to explain the results for temperature dependence of resistivity in SFMO films [10]. Temperature dependence of resistivity in valence manganites is normally described by the following equation $\rho_{\mathrm{m}} = \rho_0 + \rho_2 T^2 + \rho_{4.5} T^{4.5}$, where ρ_0

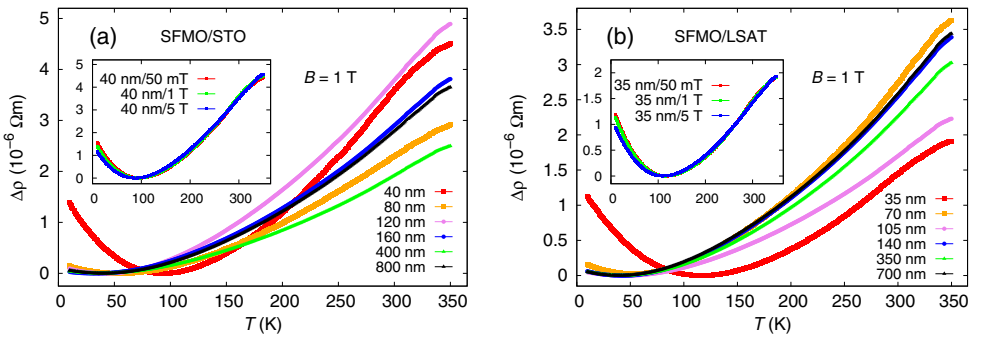

Figure 5: Temperature dependence of the resistivity change for SFMO films deposited on STO (a) and LSAT (b) substrates. Errors in resistivity are mainly due to thin film volume and measuring points. We approximate that error in resistivity change is $1 \cdot 10^{-7}\Omega$m.

describes temperature independent resistivity, which arises from grain boundries and impurities [27]. The term $\rho_2 T^2$ is accociated with the electron-electron scattering in the system [28] and $\rho_{4.5} T^{4.5}$ refers to electron magnon scattering [27]. However, this model alone does not explain semiconducting behaviour at low temperature. In the SFMO band structure, there is a gap in the majority spin band and the system can be considered as system of two spin channels connected in parallel [1, 29, 30]. Semiconducting behaviour of resistivity follows the relation $\rho_{\mathrm{sc}} = \rho_{\mathrm{d}}^{\mathrm{sc}} e^{\mathrm{E_g/kT}} + \rho_0^{\mathrm{sc}}$ where E_{g} is the energy gap of the semiconductor, $\rho_{\mathrm{d}}^{\mathrm{sc}}$ comes from electrical charge density and its temperature dependence follows the relation $\rho_{\mathrm{d}}^{\mathrm{sc}} \propto T^{-\frac{3}{2}}$. Constant ρ_0^{sc} represents the resistivity that is usually associated with impurities. Finally, the total resistivity of parallel SFMO spin channel system can be formulated as $(1/\rho_{\mathrm{tot}}) = (1/\rho_{\mathrm{sc}}) + (1/\rho_{\mathrm{m}})$ [10]. In perfect SFMO energy gap value is around 0.8 eV [31] and semiconducting behaviour is not expected. However, due to imperfections in SFMO samples energy gap in majority band is decreased and semiconducting behaviour arises.

From the fit to the resistivity data, we obtained the values for E_{g} as a fitting parameter and the error values for E_{g}. As an example, the Fig. 6(a) presents resistivity of 35 nm thick SFMO film on LSAT with the highest upturn in resistivity and the fit to the parallel spin channel model. We can see that the fitted model follows our measurements quite well, however, the model deviates from measurements in the temperature over 310 K. Parallel spin channel system model does not take into account possible effects of ferro-paramagnetic transition, which takes place at T_{C}. This explains why the used model deviates from the results and therefore we used only temperature values below 310 K for equation fitting. Also, the fitting becomes increasingly difficult with decreasing upturn, which can also be seen as larger error bars for E_{g} values in thicker films. Results for E_{g} with the error bars are presented in the inset of Fig. 6(b). E_{g} seems to be the smallest in the thinnest films below 100 nm on both substrates. These films also indicate stronger resistivity upturn at low temperatures and higher $T_{\rho\mathrm{min}}$ temperature. Our obtained values for energy gap are significantly smaller than theoretical values [31, 17]. This might due to the fact that SFMO no longer works as a perfect half metallic material.

Previous experiments have reported similar upturn in resistivity [10, 11, 15, 16]. Conducted studies suggest that strain effects to the SFMO band structure and may reduce the band gap in majority spin up band [4]. Recent theoretical work shows that both compressive and tensile strain almost linearly reduce the band gap in SFMO [17]. Also structural defects such as ASD

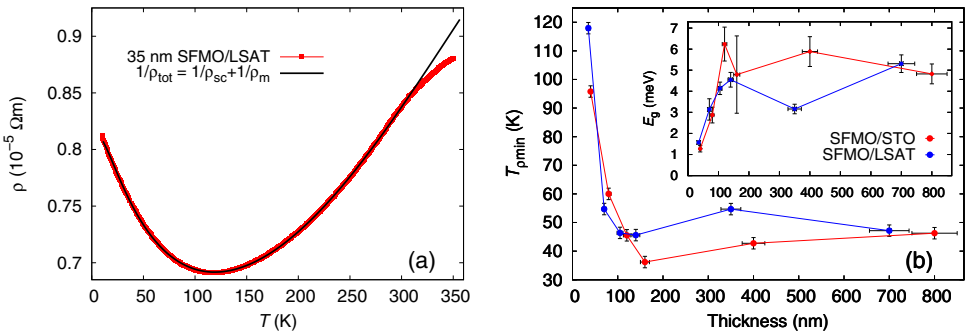

Figure 6: An example of the fit to the traditional resisitivity-temperature data of SFMO film on LSAT substrate using a model for a two spin channel system (a). (b) shows the thickness dependence of the resisitivity minimum, $T_{\rho\min}$, determined as a point where the curve crosses the zero line temperatures (main panel) and the energy gap of the semiconducting spin channel, E_g, which is given as a fitting parameter. Error bars are included for $T_{\rho\min}$, E_g and thickness.

can change the electronic structure in SFMO and reduce the band gap [19]. Our results for E_g indicate larger band gap in thicker films on both STO and LSAT. According to our structural analysis and magnetic measurements, thinner films indicated the presence of higher strain in films on STO and structural defects, like ASD, oxygen vacancies and dislocations for films on both substrates. This, through the reduction of energy gap, makes the excitation of electrons to conduction band easier and explains the lower resistivity at higher temperature, but more localization of carriers at defect sites causing greater semiconducting behaviour in the thinnest films. Both magnetic and resistive measurements show that the quality of the films on both substrates is at its best when the film thickness is around 150 nm.

4 Conclusions

We investigated structural, magnetic and resistive properties of two SFMO film series with different thicknesses deposited on STO and LSAT substrates. All the films were impurity free and fully textured. Structural properties suggested higher strain in the thinnest films grown on STO. On LSAT, the strain had a constant value through the whole thickness range. We found that the increase of film the thickness results in higher M_s and T_C. Higher semiconducting behaviour in resistivity was observed at low temperatures as an higher upturn of resistivity. The model of two spin channel system was used to determine the E_g and it appears that E_g increases with increasing film thickness. When considering magnetic and resistive properties, the results showed no clear difference between the films deposited on STO and LSAT. However, relatively small strain indicates that LSAT could be slightly better substrate option, but the larger lattice mismatch resulting higher concentration of interface defects could still prove be a disadvantage in future studies. On STO, at least 100 nm thickness, is required for the relaxed and homogenous properties for future novel technology solutions.

Acknowledgments

The Jenny and Antti Wihuri Foundation, Magnus Ehrnrooth Foundation and Kone Foundation are acknowledged for financial support.

References

[1] K.-I. Kobayashi, T. Kimura, H. Sawada, K. Terakura, Y. Tokura, Nature 395 (1998) 677.
[2] J. Santiso, A. Figueras, J. Fraxedas, Surf. Interface Anal. 33 (2002) 676.
[3] J. Raittila, T. Salminen, T. Suominen, K. Schlesier, P. Paturi, J. Phys. Chem. Solids 67 (2006) 1712.
[4] T. Fix, D. Stoeffler, S. Colis, C. Ullhaq, G. Versini, J. P. Vola, F. Huber, A. Dinia, J. Appl. Phys. 98 (2005) 023712.
[5] R. Boucher, Journal of Physics and Chemistry of Solids 66 (2005) 1020.
[6] R. Boucher, J. Magn. and Magn. Mater. 301 (2006) 251.
[7] H. Jalili, N. F. Heinig, K. T. Leung, J. Chem. Phys 132 (2010) 204701.
[8] D. Kumar, D. Kaur, Physica B 405 (2010) 3259.
[9] M. Saloaro, H. Deniz, H. Huhtinen, H. Palonen, S. Majumdar, P. Paturi, Submitted to: J. Phys.: Condens. Matter
[10] M. Saloaro, S. Majumdar, H. Huhtinen, P. Paturi, J. Phys. Cond. Mat. 24 (2012) 366003.
[11] M. Saloaro, S. Majumdar, H. Huhtinen, P. Paturi, EPJ Web of Conferences 40 (2013) 15012.
[12] A. S. Ogale, S. B. Ogale, R. Ramesh, T. Venkatesan, Appl. Phys. Lett. 75 (1999) 537.
[13] D. Stoeffler, S. Colis, Materials Science and Engineering B 126 (2006) 133.
[14] P. Paturi, M. Metsänoja, H. Huhtinen, Thin Solid Films 519 (2011) 8047.
[15] W. Westerburg, D. Reisinger, G. Jakob, Phys. Rev. B 62 (2000) R767.
[16] A. Venimadhav, F. Sher, J. P. Attfield, M. G. Blamire, J. Magn. and Magn. Mater. 269 (2004) 101.
[17] R. Lu, H. Wu, Y. Qian, E. Kan, Y. Liu, W. Tan, C. Xiao, K. Deng, Solid State Commun. 191 (2014) 70.
[18] D. Stoeffler, S. Colis, J. Phys. Cond. Mat. 17 (2005) 6415.
[19] D. Stoeffler, S. Colis, J. Magn. and Magn. Mater. 290-291 (2005) 400.
[20] T. Suominen, J. Raittila, T. Salminen, K. Schlesier, J. Linden, P. Paturi, J. Magn. and Magn. Mater. 309 (2007) 278.
[21] H. Deniz, D. Preziosi, M. Alexe, D. Hesse, C. Eisenschmidt, G. Schmidt, L. Pintilie, J. Mater. Sci. 50 (2015) 3131.
[22] J. B. Nelson, D. P. Riley, Proc. Phys. Soc. 57 (1945) 160.
[23] S. Nakamura, K. Oikawa, J. Phys. Soc. Jpn. 72 (2003) 3123.
[24] D. Jiles, D. Atherton, J. Magn. and Magn. Mater. 61 (1986) 48.
[25] H. Q. Yin, J. Zhou, R. Dass, J. Zhou, J. T. McDevitt, J. B. Goodenough, J. Appl. Phys. 87 (2000) 6761.
[26] L. Sampaio, S. da Cunha, J. Magn. and Magn. Mater. 99 (1991) 145.
[27] G. J. Snyder, R. Hiskes, S. DiCarolis, M. R. Beasley, T. H. Geballe, Phys. Rev. B 53 (1996) 14434.
[28] A. Urushibara, Y. Moritomo, T. Arima, A. Asamitsu, G. Kido, Y. Tokura, Phys. Rev. B 51 (1995) 14103.
[29] Y. Tomioka, T. Okuda, Y. Okimoto, R. Kumai, K.-I. Kobayashi, Y. Tokura, Phys. Rev. B 61 (2000) 422.
[30] H.-T. Jeng, G. Y. Guo, Phys. Rev. B 67 (2003) 094438.

[31] D. D. Sarma, P. Mahadevan, T. Saha-Dasgupta, S. Ray, A. Kumar, Phys. Rev. Lett. 85 2549